

Article

Krasnoshteinite, $\text{Al}_8[\text{B}_2\text{O}_4(\text{OH})_2](\text{OH})_{16}\text{Cl}_4 \cdot 7\text{H}_2\text{O}$, a New Microporous Mineral with a Novel Type of Borate Polyanion

Igor V. Pekov^{1,*}, Natalia V. Zubkova¹, Ilya I. Chaikovskiy², Elena P. Chirkova², Dmitry I. Belakovskiy³, Vasiliy O. Yapaskurt¹, Yana V. Bychkova¹, Inna Lykova⁴, Sergey N. Britvin^{5,6} and Dmitry Yu. Pushcharovsky¹

¹ Faculty of Geology, Moscow State University, Vorobievy Gory, 119991 Moscow, Russia; n.v.zubkova@gmail.com (N.V.Z.); yvo72@geol.msu.ru (V.O.Y.); yanab66@yandex.ru (Y.V.B.); dmitp@geol.msu.ru (D.Y.P.)

² Mining Institute, Ural Branch of the Russian Academy of Sciences, Sibirskaya str., 78a, 614007 Perm, Russia; ilya@mi-perm.ru (I.I.C.); zaitseva59@mail.ru (E.P.C.)

³ Fersman Mineralogical Museum, Russian Academy of Sciences, Leninsky Prospekt 18-2, 119071 Moscow, Russia; dmzvr@mail.ru

⁴ Canadian Museum of Nature, 240 McLeod St, Ottawa, ON K2P 2R1, Canada; ilykova@nature.ca

⁵ Department of Crystallography, St. Petersburg State University, Universitetskaya nab. 7/9, 199034 St. Petersburg, Russia; sbritvin@gmail.com

⁶ Kola Science Centre, Russian Academy of Sciences, Fersman Street 14, 184209 Apatity, Russia

* Correspondence: igorpekov@mail.ru

Received: 6 April 2020; Accepted: 12 April 2020; Published: 15 April 2020



Abstract: A new mineral, krasnoshteinite ($\text{Al}_8[\text{B}_2\text{O}_4(\text{OH})_2](\text{OH})_{16}\text{Cl}_4 \cdot 7\text{H}_2\text{O}$), was found in the Verkhnekamskoe potassium salt deposit, Perm Krai, Western Urals, Russia. It occurs as transparent colourless tabular to lamellar crystals embedded up to $0.06 \times 0.25 \times 0.3$ mm in halite-carnallite rock and is associated with dritsite, dolomite, magnesite, quartz, baryte, kaolinite, potassic feldspar, congolite, members of the goyazite–woodhouseite series, fluorite, hematite, and anatase. $D_{\text{meas}} = 2.11$ (1) and $D_{\text{calc}} = 2.115$ g/cm³. Krasnoshteinite is optically biaxial (+), $\alpha = 1.563$ (2), $\beta = 1.565$ (2), $\gamma = 1.574$ (2), and $2V_{\text{meas}} = 50$ (10)°. The chemical composition (wt.%; by combination of electron microprobe and ICP-MS; H₂O calculated from structure data) is: B₂O₃ 8.15, Al₂O₃ 46.27, SiO₂ 0.06, Cl 15.48, H₂O_{calc.} 33.74, –O=Cl –3.50, totalling 100.20. The empirical formula calculated based on O + Cl = 33 *apfu* is $(\text{Al}_{7.87}\text{Si}_{0.01})_{\Sigma 7.88}[\text{B}_{2.03}\text{O}_4(\text{OH})_2][(\text{OH})_{15.74}(\text{H}_2\text{O})_{0.26}]_{\Sigma 16}[(\text{Cl}_{3.79}(\text{OH})_{0.21})_{\Sigma 4} \cdot 7\text{H}_2\text{O}$. The mineral is monoclinic, $P2_1$, $a = 8.73980$ (19), $b = 14.4129$ (3), $c = 11.3060$ (3) Å, $\beta = 106.665$ (2)°, $V = 1364.35$ (5) Å³, and $Z = 2$. The crystal structure of krasnoshteinite (solved using single-crystal data, $R_1 = 0.0557$) is unique. It is based upon corrugated layers of Al-centered octahedra connected via common vertices. BO₃ triangles and BO₂(OH)₂ tetrahedra share a common vertex, forming insular $[\text{B}_2\text{O}_4(\text{OH})_2]^{4-}$ groups (this is a novel borate polyanion) which are connected with Al-centered octahedra via common vertices to form the aluminoborate pseudo-framework. The structure is microporous, zeolite-like, with a three-dimensional system of wide channels containing Cl[−] anions and weakly bonded H₂O molecules. The mineral is named in honour of the Russian mining engineer and scientist Arkadiy Evgenievich Krasnoshtein (1937–2009). The differences in crystal chemistry and properties between high-temperature and low-temperature natural Al borates are discussed.

Keywords: krasnoshteinite; zeolite-like borate; hydrous aluminum chloroborate; new mineral; crystal structure; microporous crystalline material; evaporitic salt rock; Verkhnekamskoe potassium salt deposit; Perm Krai

1. Introduction

Boron is a rare chemical element in nature; its average content in the upper continental crust of the Earth is 0.0011 wt.% [1]. Despite its rarity, boron demonstrates diverse and complicated mineralogy and mineral crystal chemistry. Three hundred minerals with species-defining B are known, including 160 borates and oxoborates [2], and some of these minerals form huge and sometimes extremely rich deposits. Unusual geochemical and mineralogical features of boron are due to its very bright crystal chemical individuality which causes strong ability to separate from other elements in crystal structures and form very specific, unique structural units [3,4]. Unlike boron, aluminum is one of the most abundant elements in the lithosphere, however, natural Al borates are not numerous (only twelve borate and oxoborate minerals with species-defining Al are known: see Discussion) and are classified as rare minerals.

In the present article, we characterize the new mineral species krasnoshteinite (Cyrillic: красноштейнит), a hydrous aluminum chloroborate, and its unusual crystal structure. The mineral is named in honour of the Russian mining engineer and scientist, corresponding member of the Russian Academy of Sciences, Arkadiy Evgenievich Krasnoshtein (1937–2009), an outstanding specialist in the mining of potassium salts who made a great contribution to the exploitation of underground mines at the Verkhnekamskoe deposit. Dr. Krasnoshtein was the founder (1988) and first director of the Mining Institute of the Ural Branch of the Russian Academy of Sciences in Perm. Both the new mineral and its name have been approved by the Commission on New Minerals, Nomenclature and Classification of the International Mineralogical Association, IMA No. 2018-077.

The type specimen of krasnoshteinite was deposited in the systematic collection of the Fersman Mineralogical Museum of the Russian Academy of Sciences (Moscow, Russia), under the catalogue number 96274.

2. Materials and Methods

2.1. Occurrence, General Appearance, Physical Properties and Optical Data

Krasnoshteinite was found in the core of the borehole #2001, with a depth of 247.6–248 m, drilled in the Romanovski area (30 km south of the city of Berezniki) of the Verkhnekamskoe potassium salt deposit, Perm Krai, Western Urals, Russia. The general data on this well-known. Huge deposits are given in monographs [5,6]. Krasnoshteinite occurs in halite-carnallite rock and is associated with dritsite ($\text{Li}_2\text{Al}_4(\text{OH})_{12}\text{Cl}_2 \cdot 3\text{H}_2\text{O}$) [7], dolomite, magnesite, quartz, Sr-bearing baryte, kaolinite, potassic feldspar, congolite, members of the goyazite $\text{SrAl}_3(\text{PO}_4)(\text{PO}_3\text{OH})(\text{OH})_6$ –woodhouseite $\text{CaAl}_3(\text{PO}_4)(\text{SO}_4)(\text{OH})_6$ series, fluorite, hematite, and anatase. The new mineral was probably formed as a result of diagenetic or post-diagenetic processes in halite-carnallite evaporitic rock of the Layer E of the Verkhnekamskoe deposit.

Krasnoshteinite occurs as separate tabular to lamellar crystals of up to $0.06 \times 0.25 \times 0.3$ mm (Figure 1a,b) and their parallel intergrowths (Figure 1c) embedded in carnallite and halite. In some cases, tiny crystals of krasnoshteinite overgrow its larger crystal in random orientations to form a crystal cluster (Figure 1d). Samples shown in Figure 1 were separated after dissolution of a host halite-carnallite rock in water.

Crystals of krasnoshteinite are flattened on the *ab* plane. The pedions {010} and {0-10} and the pinacoid {100} are major lateral faces of the tabular crystals. The surface of the most developed “face” of a crystal is typically complicated, rough, and demonstrating coarse or/and fine striation along {100} (Figure 1); it is usually composed by several poorly formed faces belonging to the *0kl* zone.

Krasnoshteinite is a transparent colorless mineral with a white streak and vitreous luster. It is brittle, with a Mohs hardness is ca. of 3. Krasnoshteinite demonstrates perfect cleavage on {010} and an imperfect cleavage on {100}. A fracture is stepped (observed under the microscope). The mineral is non-fluorescent in the ultraviolet light. The density measured by flotation in heavy liquids (bromofom

+ dimethylformamide) is $2.11 (1) \text{ g/cm}^3$, and the density calculated using the empirical formula and the unit-cell parameters determined from single-crystal X-ray diffraction data is 2.115 g/cm^3 .

In plane polarized light, krasnoshteinite is colorless and non-pleochroic. It is optically biaxial (+), $\alpha = 1.563 (2)$, $\beta = 1.565 (2)$, $\gamma = 1.574 (2)$ (589 nm). $2V$ (meas.) = $50 (10)^\circ$ and $2V$ (calc.) = 51° . Dispersion of optical axes is distinct, $r > v$. Optical orientation is: $Y = b$, and $X = a$.

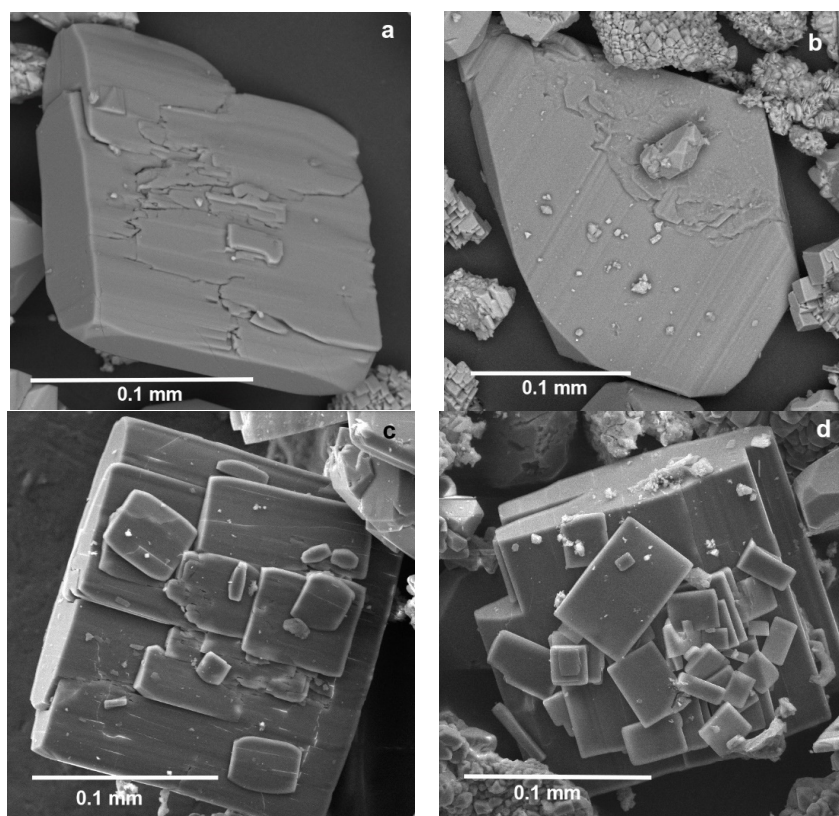


Figure 1. Separate crystals (a,b) and crystal clusters ((c,d): small crystals overgrow large crystal) of krasnoshteinite. Blocky crystals of dolomite and distorted quartz crystal are observed in (b).

2.2. Chemical Composition

The chemical composition of krasnoshteinite was studied using a Jeol JSM-6480LV scanning electron microscope equipped with an INCA-Wave 500 wavelength-dispersive spectrometer (Laboratory of Analytical Techniques of High Spatial Resolution, Dept. of Petrology, Moscow State University). Electron microprobe analyses were obtained in the wavelength-dispersive spectroscopy mode (20 kV and 20 nA; the electron beam was rastered to the $5 \times 5 \mu\text{m}$ area to avoid damage of the highly hydrated mineral) and gave contents of Al, Si, O, and Cl. The standards used were: Al_2O_3 (Al), wollastonite (Si), $\text{YAl}_3(\text{BO}_3)_4$ (O), and NaCl (Cl). The contents of other elements with atomic numbers higher than 8 are below detection limits.

The presence of significant amount of chlorine in krasnoshteinite prevents the quantitative determination of boron by electron microprobe, due to the overlap of X-ray emission lines of the K series of B with L lines of Cl. The boron content was determined using ICP-MS. The measurements were carried out with the Element-2 (Thermo Fisher Scientific) instrument which has high resolution (that avoids interference of components) and sensitivity. Several crystals of the mineral were dissolved in 10 cm^3 of 3% HNO_3 solution (Merck, Suprapur[®]) in deionized water (EasyPure). Since the mass of the mineral was too small for accurate weighing, we have determined contents of B and Al in relative units and further used averaged Al content, obtained by electron microprobe, for B content calculation. The obtained value is in good agreement with the boron content determined from the crystal structure refinement. Contents of Li and Be in krasnoshteinite are below detection limits.

H₂O was not analysed because of the paucity of material. Hydrogen (H₂O) content was calculated based on the structure data (see below) and taking into account the charge balance requirement. The analytical total is close to 100 wt.% (Table 1) that demonstrates a good agreement between electron microprobe data for Al, Si, O, and Cl, ICP-MS data for B and calculated value for H. The correctness of the obtained chemical data was also confirmed by the superior value of the Gladstone–Dale compatibility index [8]: $1 - (K_p/K_c) = 0.003$ (superior) with measured density value, or 0.006 (superior) with calculated density value.

CO₂ was not analysed because the structure data showed the absence of this constituent. The absence of gas release in HCl (see below) also indicated that krasnoshteinite does not contain carbonate groups.

2.3. Single-Crystal X-ray Diffraction and Crystal Structure Determination

Single-crystal X-ray diffraction data were collected by means of an Xcalibur S CCD diffractometer (Dept. of Crystallography and Crystal Chemistry, Faculty of Geology, Moscow State University) operated at 40 kV and 50 mA using MoK α radiation. A full sphere of three-dimensional data was collected. Data reduction was performed using CrysAlisPro Version 1.171.37.35 [9]. The data were corrected for Lorentz factor and polarization effects. The crystal structure was solved and refined with the ShelX program package using direct methods [10].

2.4. Powder X-ray Diffraction

Powder X-ray diffraction data were collected by means of a Rigaku R-Axis Rapid II diffractometer (XRD Resource Center, St. Petersburg State University) equipped with a rotating anode X-ray source and a curved image plate detector (Debye-Scherrer geometry, $d = 127.4$ mm, CoK α , $\lambda = 1.79021$ Å). The data were integrated using the software package Osc2Tab/SQRay [11]. The unit-cell parameters were refined from the powder data using the Pawley method and Topas software [12].

3. Results

3.1. Chemical Data

Chemical composition of krasnoshteinite is given in Table 1. The empirical formula calculated on the basis of O + Cl = 33 atoms per formula unit is H_{32.47}Al_{7.87}Si_{0.01}B_{2.03}Cl_{3.79}O_{29.71} or, after recalculation of the anionic part and taking into account crystal-structure data, (Al_{7.87}Si_{0.01}) Σ _{7.88}[B_{2.03}O₄(OH)₂][(OH)_{15.74}(H₂O)_{0.26}] Σ ₁₆[(Cl_{3.79}(OH)_{0.21}] Σ ₄·7H₂O. The ideal formula is Al₈[B₂O₄(OH)₂](OH)₁₆Cl₄·7H₂O, which requires Al 24.65, B 2.47, Cl 16.19, H 3.69, O 53.00, total 100 wt.%, or, in oxides, Al₂O₃ 46.58, B₂O₃ 7.95, H₂O 32.93, Cl 16.19, –O=Cl –3.65, total 100 wt.%.

Table 1. Chemical composition (in wt.%) of krasnoshteinite in elements and in oxides (Al, Si, Cl, and O: average data for 7 spot electron-microprobe analyses).

Data in Elements, with Measured O Content				Data Recalculated in Oxides	
Constituent	Wt.%	Range	Stand. Dev.	Constituent	Wt.%
B	2.53			B ₂ O ₃	8.15
Al	24.49	23.79–24.96	0.41	Al ₂ O ₃	46.27
Si	0.03	0.02–0.05	0.01	SiO ₂	0.06
Cl	15.48	15.01–16.69	0.59	Cl	15.48
H(calc.)	3.75			H ₂ O (calc.)	33.74
O	53.92	52.43–56.62	1.42	–O=Cl	–3.50
Total	100.20			Total	100.20

Krasnoshteinite is insoluble in water and slowly dissolves in cold diluted HCl without effervescence. The obtained solution shows characteristic color reaction, with quinalizarin clearly indicating boron presence.

3.2. Single-Crystal X-ray Diffraction and Crystal Structure Determination

The single-crystal X-ray diffraction data were indexed in the $P2_1$ space group with the following unit-cell parameters: $a = 8.73980$ (19), $b = 14.4129$ (3), $c = 11.3060$ (3) Å, $\beta = 106.665$ (2)°, and $V = 1364.35$ (5) Å³ (Table 2). Details on data collection and structure refinement are also given in Table 2. The final structure refinement converged to $R_1 = 0.0557$ for 6142 unique observed reflections with $I > 2\sigma(I)$. The H atoms of OH groups and H₂O molecules were located from the difference Fourier synthesis. The studied crystal is microtwinning with the inversion center as a twin operation: twinning by merohedry Class I [13] with the twin domain ratio of 68/32. Coordinates and equivalent thermal displacement parameters of atoms are given in Table 3, selected interatomic distances in Table 4, and H-bonding in Table 5. Other crystal structure information for krasnoshteinite has been deposited with the Editors and is available as Supplementary Materials (see below): anisotropic displacement parameters of non-hydrogen atoms in the structure are presented in Table S1 and bond valence calculations in Table S2; crystallographic information file (CIF) is given as a separate Supplementary Material. Bond-valence parameters for Al-O and B-O were taken from [14] and for H-bonding from [15,16].

Table 2. Crystal data, data collection information and structure refinement details for krasnoshteinite.

Formula	Al ₈ [B ₂ O ₄ (OH) ₂](OH) ₁₆ Cl ₄ ·7H ₂ O
Formula weight	875.52
Temperature, K	293 (2)
Radiation and wavelength, Å	MoKα; 0.71073
Crystal system, space group, Z	Monoclinic, $P2_1$, 2
Unit cell dimensions, Å/°	$a = 8.73980$ (19) $b = 14.4129$ (3) $\beta = 106.665$ (2) $c = 11.3060$ (3)
V , Å ³	1364.35 (5)
Absorption coefficient μ , mm ⁻¹	0.809
F_{000}	892
Crystal size, mm	0.06 × 0.16 × 0.17
Diffractometer	Xcalibur S CCD
θ range for data collection, °/Collection mode	2.81 – 28.28/full sphere
Index ranges	$-11 \leq h \leq 11$, $-19 \leq k \leq 19$, $-15 \leq l \leq 15$
Reflections collected	23,807
Independent reflections	6773 ($R_{\text{int}} = 0.0759$)
Independent reflections with $I > 2\sigma(I)$	6142
Data reduction	CrysAlisPro, Agilent Technologies, v. 1.171.37.35 [9] multi-scan
Absorption correction	Empirical absorption correction using spherical harmonics, implemented in SCALE3 ABSPACK scaling algorithm
Structure solution	direct methods
Refinement method	full-matrix least-squares on F^2
Number of refined parameters	485
Final R indices [$I > 2\sigma(I)$]	$R_1 = 0.0557$, $wR_2 = 0.1157$
R indices (all data)	$R_1 = 0.0633$, $wR_2 = 0.1196$
GooF	1.107
Largest diff. peak and hole, e/Å ³	0.60 and -0.56

Table 3. Coordinates and equivalent displacement parameters (U_{eq} , in \AA^2) of atoms in krasnoshteinite.

Site	X	Y	Z	U_{eq} *
Al1	0.16497(17)	0.29061(10)	0.29761(12)	0.0100(3)
Al2	−0.15081(17)	0.71563(9)	−0.04927(12)	0.0097(3)
Al3	0.11906(16)	0.67894(10)	−0.16964(12)	0.0098(3)
Al4	−0.15717(16)	0.11133(9)	−0.07805(12)	0.0089(3)
Al5	0.50122(18)	0.16162(11)	−0.01146(13)	0.0101(2)
Al6	0.11383(16)	0.13955(10)	−0.19674(12)	0.0103(3)
Al7	0.16655(16)	0.52591(10)	0.31878(12)	0.0094(3)
Al8	0.00144(18)	0.65411(11)	0.51556(12)	0.0112(3)
B1	0.2145(5)	0.4153(4)	0.0964(4)	0.0102(9)
B2	0.7283(6)	−0.0017(4)	0.0864(5)	0.0123(10)
Cl1	0.62010(14)	0.41682(12)	0.28131(13)	0.0305(3)
Cl2	0.24073(14)	0.91650(11)	0.04320(14)	0.0318(3)
Cl3	0.61509(17)	0.82518(11)	0.35183(13)	0.0321(3)
Cl4	0.5240(2)	0.57208(11)	0.64519(13)	0.0371(4)
O1	0.1226(4)	0.1723(2)	0.2021(3)	0.0096(6)
H1	0.182(5)	0.122(2)	0.247(4)	0.012
O2	0.3923(4)	0.2700(3)	0.3509(3)	0.0175(8)
H2A	0.444(5)	0.2119(17)	0.369(5)	0.021
H2B	0.451(5)	0.302(3)	0.305(4)	0.021
O3	0.1966(3)	0.4058(3)	0.3715(3)	0.0145(6)
H3	0.232(5)	0.402(4)	0.4585(10)	0.017
O4	0.0817(4)	0.7234(2)	−0.0141(3)	0.0103(6)
H4	0.128(6)	0.7797(19)	0.022(4)	0.012
O5	0.3314(4)	0.7079(2)	−0.1198(3)	0.0142(7)
H5	0.341(6)	0.7694(14)	−0.144(4)	0.017
O6	−0.1336(4)	0.7504(2)	0.1100(3)	0.0112(6)
H6	−0.149(6)	0.8122(14)	0.133(4)	0.013
O7	0.0760(4)	0.1003(2)	−0.0385(3)	0.0109(7)
H7	0.137(5)	0.047(2)	−0.008(4)	0.013
O8	0.6348(4)	0.1519(3)	−0.1168(3)	0.0143(7)
H8	0.588(6)	0.165(4)	−0.2011(16)	0.017
O9	0.3603(4)	0.1780(2)	0.0857(3)	0.0104(6)
H9	0.396(6)	0.146(3)	0.161(2)	0.012
O10	−0.0590(4)	0.2960(2)	0.2401(3)	0.0119(7)
H10	−0.113(5)	0.3394(7)	0.179(2)	0.014
O11	−0.1825(4)	0.8288(2)	−0.1385(3)	0.0124(7)
O12	0.5632(4)	0.0394(2)	0.0507(3)	0.0130(7)
H12	0.479(4)	−0.003(3)	0.043(5)	0.016
O13	0.8084(4)	−0.0053(2)	−0.1569(3)	0.0092(6)
O14	0.1514(4)	0.2235(2)	0.4336(3)	0.0124(7)

Table 3. Cont.

Site	X	Y	Z	U_{eq} *
H14	0.223(4)	0.246(3)	0.5072(14)	0.015
O15	0.7339(3)	−0.0820(3)	0.0047(3)	0.0143(6)
O16	0.5396(4)	0.7888(2)	0.0675(3)	0.0165(7)
H16A	0.625(4)	0.829(3)	0.065(5)	0.020
H16B	0.478(5)	0.824(3)	0.108(4)	0.020
O17	0.0990(4)	0.6243(2)	0.6804(3)	0.0120(7)
H17	0.144(5)	0.5646(16)	0.6811(15)	0.014
O18	0.7769(4)	−0.0354(3)	0.2134(3)	0.0201(7)
H18	0.706(5)	−0.070(3)	0.245(4)	0.024
O19	−0.1261(4)	0.1448(2)	0.7681(3)	0.0092(6)
H19	−0.172(6)	0.198(2)	0.723(4)	0.011
O20	−0.1619(4)	0.0707(2)	0.0752(3)	0.0088(6)
O21	0.3296(4)	0.1147(2)	−0.1411(3)	0.0121(7)
H21	0.364(6)	0.0579(19)	−0.166(4)	0.015
O22	0.1002(4)	0.1859(2)	0.6494(3)	0.0147(7)
H22	0.180(4)	0.228(3)	0.642(5)	0.018
O23	0.0542(4)	0.0215(2)	0.7411(3)	0.0123(7)
H23	0.106(5)	−0.030(2)	0.717(4)	0.015
O24	0.1359(5)	0.0438(3)	0.4965(3)	0.0214(8)
H24A	0.214(5)	0.022(4)	0.567(2)	0.026
H24B	0.150(6)	0.010(3)	0.429(3)	0.026
O25	−0.1540(4)	0.0819(2)	0.5351(3)	0.0145(7)
H25	−0.248(4)	0.088(4)	0.470(3)	0.017
O26	0.3966(4)	0.5521(2)	0.3674(3)	0.0173(8)
H26A	0.458(5)	0.502(2)	0.352(4)	0.021
H26B	0.444(5)	0.566(3)	0.4523(16)	0.021
O27	−0.1362(4)	0.2617(3)	0.4649(3)	0.0230(8)
H27A	−0.134(6)	0.308(3)	0.408(4)	0.028
H27B	−0.223(4)	0.274(3)	0.496(4)	0.028
O28	0.7250(5)	0.2946(3)	0.6403(4)	0.0354(10)
H28A	0.617(3)	0.289(4)	0.641(6)	0.043
H28B	0.760(6)	0.351(3)	0.684(5)	0.043
O29	0.1131(6)	0.9559(4)	0.2765(5)	0.0571(15)
H29A	0.127(8)	0.952(5)	0.197(3)	0.069
H29B	0.010(5)	0.930(6)	0.269(6)	0.069

* The positions of H atoms were located from the difference Fourier map and refined with O-H and H-H distances softly restrained to 0.95(1) and 1.50(1) Å, respectively, to hold near-optimal geometry. U_{iso} (H) = 1.2 U_{eq} (O).

Table 4. Selected interatomic distances (Å) in the structure of krasnoshteinite.

Al1 - O3	1.843(4)	Al5 - O5	1.882(4)
- O14	1.849(3)	- O9	1.885(3)
- O10	1.879(3)	- O21	1.896(3)
- O2	1.927(4)	- O8	1.897(3)
- O11	1.929(3)	- O12	1.916(4)
- O1	1.996(3)	- O16	1.939(4)
<Al1 - O>	1.904	<Al5 - O>	1.903
Al2 - O6	1.833(3)	Al6 - O22	1.835(3)
- O9	1.839(3)	- O21	1.844(3)
- O11	1.896(3)	- O6	1.857(3)
- O1	1.918(3)	- O23	1.858(4)
- O7	1.951(3)	- O7	1.992(3)
- O4	1.959(3)	- O19	2.021(3)
<Al2 - O>	1.899	<Al6 - O>	1.901
Al3 - O5	1.827(4)	Al7 - O3	1.825(4)
- O17	1.831(3)	- O23	1.853(3)
- O20	1.867(3)	- O25	1.869(3)
- O10	1.875(4)	- O19	1.956(3)
- O4	1.984(3)	- O13	1.956(3)
- O1	2.040(3)	- O26	1.963(4)
<Al3 - O>	1.904	<Al7 - O>	1.904
Al4 - O8	1.839(3)	Al8 - O17	1.864(3)
- O20	1.841(3)	- O22	1.878(3)
- O13	1.886(3)	- O14	1.886(3)
- O19	1.898(3)	- O25	1.905(4)
- O4	1.932(3)	- O27	1.921(4)
- O7	1.963(3)	- O24	1.973(4)
<Al4 - O>	1.893	<Al8 - O>	1.905
B1 - O15	1.344(5)	B2 - O20	1.448(6)
- O13	1.377(7)	- O18	1.459(6)
- O11	1.392(6)	- O15	1.490(6)
<B1 - O>	1.371	- O12	1.504(6)
		<B2 - O>	1.475

Table 5. Hydrogen-bond geometry (Å, °) in the structure of krasnoshteinite.

D - H...A	D - H	H...A	D...A	∠(D - H...A)
O1 - H1...O29		2.52(4)	3.237(7)	133(4)
O1 - H1...Cl4	0.946(10)	2.61(3)	3.398(3)	141(4)
O2 - H2A...Cl4	0.947(10)	2.05(2)	2.942(4)	157(5)
O2 - H2B...Cl1	0.947(10)	2.28(2)	3.156(4)	153(4)
O3 - H3...Cl3	0.945(10)	2.44(3)	3.300(3)	151(5)
O4 - H4...Cl2	0.947(10)	2.185(19)	3.096(4)	161(4)
O5 - H5...Cl1	0.940(10)	2.71(2)	3.609(4)	161(4)
O6 - H6...O15		2.15(4)	2.794(5)	124(4)
O6 - H6...O18	0.946(10)	2.533(15)	3.468(5)	170(4)
O7 - H7...Cl2	0.945(10)	2.093(14)	3.030(4)	171(5)
O8 - H8...O26	0.942(10)	2.52(5)	3.119(5)	121(4)
O9 - H9...Cl4	0.943(10)	2.352(11)	3.294(3)	177(4)
O10 - H10...Cl2	0.948(10)	2.684(17)	3.589(3)	160(3)
O12 - H12...Cl2	0.946(10)	2.380(15)	3.309(3)	168(4)
O14 - H14...Cl3	0.943(10)	2.134(12)	3.059(3)	167(3)
O16 - H16A...O15	0.949(10)	1.84(2)	2.747(5)	158(5)

Table 5. Cont.

D – H...A	D – H	H...A	D...A	$\angle(\text{D} - \text{H} \cdots \text{A})$
O16 - H16A...O6	0.949(10)	2.32(4)	2.812(5)	111(3)
O16 - H16B...Cl2	0.952(10)	2.40(4)	3.143(4)	135(4)
O16 - H16B...Cl3	0.952(10)	2.67(5)	3.135(4)	111(3)
O17 - H17...O18	0.944(10)	1.873(13)	2.677(5)	141.5(19)
O18 - H18...Cl3	0.945(10)	2.22(2)	3.123(4)	160(5)
O19 - H19...O28	0.946(10)	1.770(12)	2.714(5)	175(5)
O21 - H21...Cl1	0.941(10)	2.441(18)	3.353(4)	163(4)
O22 - H22...Cl3	0.946(10)	2.259(12)	3.200(4)	173(4)
O23 - H23...Cl1	0.944(10)	2.51(3)	3.295(3)	140(4)
O23 - H23...O10		2.61(4)	3.257(4)	126(4)
O24 - H24A...Cl1	0.940(10)	2.43(2)	3.337(4)	161(4)
O24 - H24B...O29	0.942(10)	1.835(16)	2.747(6)	162(4)
O25 - H25...Cl4	0.941(10)	2.40(2)	3.294(4)	160(4)
O26 - H26A...Cl1	0.951(10)	2.187(18)	3.107(4)	163(5)
O26 - H26B...Cl4	0.952(10)	2.092(16)	3.030(4)	168(5)
O27 - H27A...O10	0.935(10)	2.19(4)	2.853(5)	128(4)
O27 - H27A...Cl1		2.71(4)	3.363(4)	128(3)
O27 - H27B...O28	0.940(10)	1.84(3)	2.648(5)	142(4)
O28 - H28A...Cl3	0.951(10)	2.12(2)	3.031(4)	161(5)
O28 - H28B...O29	0.951(10)	1.86(3)	2.745(7)	154(5)
O29 - H29A...Cl2	0.946(10)	2.29(3)	3.196(6)	160(6)
O29 - H29B...O18	0.951(10)	2.02(6)	2.820(6)	141(7)

3.3. Powder X-ray Diffraction

The indexed powder X-ray diffraction data are given in Table S3 in Supplementary Materials (see below). The powder X-ray diffraction pattern of krasnoshteinite is unique and can be used as a good diagnostic tool of the mineral. The parameters of a monoclinic unit cell refined from the powder data are as follows: $a = 8.740$ (4), $b = 14.409$ (4), $c = 11.316$ (4) Å, $\beta = 106.58$ (3)°, and $V = 1366$ (1) Å³.

4. Discussion

The crystal structure of krasnoshteinite (Figure 2) is unique. It is based upon the (010) corrugated layers of Al-centered octahedra connected via common vertices to form a pseudo-framework. There are eight crystallographically non-equivalent octahedrally coordinated Al sites: Al(1) and Al(7) cations center octahedra $\text{AlO}(\text{OH})_4(\text{OH}_2)$, Al(2,3) – $\text{AlO}(\text{OH})_5$, Al(4) – $\text{AlO}_2(\text{OH})_4$, Al(5) – $\text{Al}(\text{OH})_5(\text{OH}_2)$, Al(6) – $\text{Al}(\text{OH})_6$, and Al(8) – $\text{Al}(\text{OH})_4(\text{OH}_2)_2$. These Al-centered octahedra play different structural roles. Al(1–4)- and Al(6,7)-centered octahedra share edges to form six-membered clusters. Al(8)-centered octahedra link adjacent clusters along the c axis sharing two corners with each cluster, while Al(5)-centered octahedra play the same role linking the clusters along the a axis to form octahedral layers (Figure 3a). Adjacent layers are connected via the common O(3) vertex of Al(7)- and Al(1)-centered octahedra, forming the three-dimensional octahedral motif.

Boron atoms occupy two crystallographically non-equivalent sites and center B(1)O₃ triangles and B(2)O₂(OH)₂ tetrahedra, which share a common vertex to form insular $[\text{B}_2\text{O}_4(\text{OH})_2]^{4-}$ groups (Figure 3b). According to the classification of fundamental building blocks (FBB) in borates [17,18], FBB in krasnoshteinite is $1\Delta\Box:\Delta\Box$, i.e., the block with one triangle and one tetrahedron sharing corner. Krasnoshteinite is the first borate with such FBBs. These groups are connected with clusters of Al-centered octahedra via common vertices. Thus, a BO₃ triangle shares one O vertex with a

B-centered tetrahedron, one vertex with two Al-centered octahedra [Al(4) and Al(7)] of the layer, and one vertex with Al(1)- and Al(2)-centered octahedra of an adjacent layer (thus reinforcing the linkage between neighboring octahedral layers). A $\text{BO}_2(\text{OH})_2$ tetrahedron shares one O vertex with a BO_3 triangle, one O vertex with two Al-centered octahedra [Al(3) and Al(4)], and one O=OH vertex with a Al(5)-centered octahedron; all Al(3,4,5) octahedra belong to the same layer. The resultant aluminoborate pseudo-framework contains three-membered [2B + Al] rings. Such Al-B-O units are known in the porous aluminoborate frameworks as being crucial to stabilizing them [19–21]. The same configuration of the three-membered [2B + Al] ring was described in the crystal structures of satimolite, $\text{KNa}_2(\text{Al}_5\text{Mg}_2)[\text{B}_{12}\text{O}_{18}(\text{OH})_{12}](\text{OH})_6\text{Cl}_4 \cdot 4\text{H}_2\text{O}$ [22], and synthetic porous Al borates, PKU-3 $\text{H}_{24.3}\text{Al}_9\text{B}_{18}\text{O}_{51}\text{Cl}_{3.3} \cdot 6.8\text{H}_2\text{O}$ [23] and PKU-8 $(\text{H}_{18}\text{Al}_7\text{B}_{12}\text{O}_{36})\text{Cl}_3(\text{NaCl})_{2.4} \cdot 6.5\text{H}_2\text{O}$ [19].

The aluminoborate pseudo-framework in krasnoshteinite is microporous and zeolite-like (Figure 2). The three-dimensional system of wide channels contains Cl^- anions and H_2O molecules. Together with OH groups and H_2O molecules belonging to Al- and B-centered polyhedra, they form a complicated system of hydrogen bonds (Table 5).

Among 160 natural borates and oxoborates, known to date as valid mineral species, only twelve minerals contain species-defining Al, namely aluminomagnesiohulsite, $(\text{Mg},\text{Fe}^{2+})_2(\text{Al},\text{Mg},\text{Sn})(\text{BO}_3)_2$; jeremejevite, $\text{Al}_6(\text{BO}_3)_5(\text{F},\text{OH})_3$; johachidolite, CaAlB_3O_7 ; krasnoshteinite, $\text{Al}_8[\text{B}_2\text{O}_4(\text{OH})_2](\text{OH})_{16}\text{Cl}_4 \cdot 7\text{H}_2\text{O}$; londonite, $\text{CsAl}_4\text{Be}_4\text{B}_{12}\text{O}_{28}$; mengxianminite, $(\text{Ca},\text{Na})_2\text{Sn}_2(\text{Mg},\text{Fe})_3\text{Al}_8[(\text{BO}_3)(\text{BeO}_4)\text{O}_6]_2$; painite, $\text{CaZrAl}_9(\text{BO}_3)_2\text{O}_{15}$; peprossiite-(Ce), $\text{CeAl}_2\text{B}_3\text{O}_9$; pseudosinhalite, $\text{Mg}_2\text{Al}_3\text{O}(\text{BO}_4)_2(\text{OH})$; rhodizite, $\text{KAl}_4\text{Be}_4\text{B}_{12}\text{O}_{28}$; satimolite, $\text{KNa}_2(\text{Al}_5\text{Mg}_2)[\text{B}_{12}\text{O}_{18}(\text{OH})_{12}](\text{OH})_6\text{Cl}_4 \cdot 4\text{H}_2\text{O}$; and sinhalite, $\text{MgAl}(\text{BO}_4)$ [2]. Satimolite and krasnoshteinite are low-temperature (LT) borates formed in evaporitic rocks, whereas the other ten minerals are known only in high-temperature (HT) geological formations: granitic pegmatites, HT metamorphic or metasomatic rocks, or post-volcanic HT assemblages. These HT Al borates and oxoborates do not contain H_2O molecules and have compact crystal structures that cause high hardness and mechanical and chemical stability in the majority of them. Data on the Mohs hardness of peprossiite-(Ce) and pseudosinhalite are absent in literature, aluminomagnesiohulsite has the Mohs hardness value of 6, and jeremejevite, johachidolite, londonite, mengxianminite, painite, rhodizite, and sinhalite demonstrate the Mohs hardness values between 7 to 8 [24]. All ten minerals have crystal structures with only one type of B-centered polyhedra, BO_3 triangles [aluminomagnesiohulsite, jeremejevite, mengxianminite, and painite], or BO_4 tetrahedra [johachidolite, londonite, peprossiite-(Ce), pseudosinhalite, rhodizite, and sinhalite], without OH groups coordinating B [25]. In LT formations, the crystal chemistry and properties of borate minerals with species-defining Al change drastically. Satimolite and krasnoshteinite are highly hydrated chloroborates which have low Mohs hardness values, 2 (satimolite) or 3 (krasnoshteinite), and dissolve even in diluted HCl. They contain complex borate polyanions composed of both B-centered triangles and tetrahedra with OH groups which participate in the tetrahedra. The structures of both satimolite and krasnoshteinite are microporous and zeolite-like. Thus, under LT conditions, aluminum octahedra in borates became a building unit of open-work aluminoborate structure motifs.

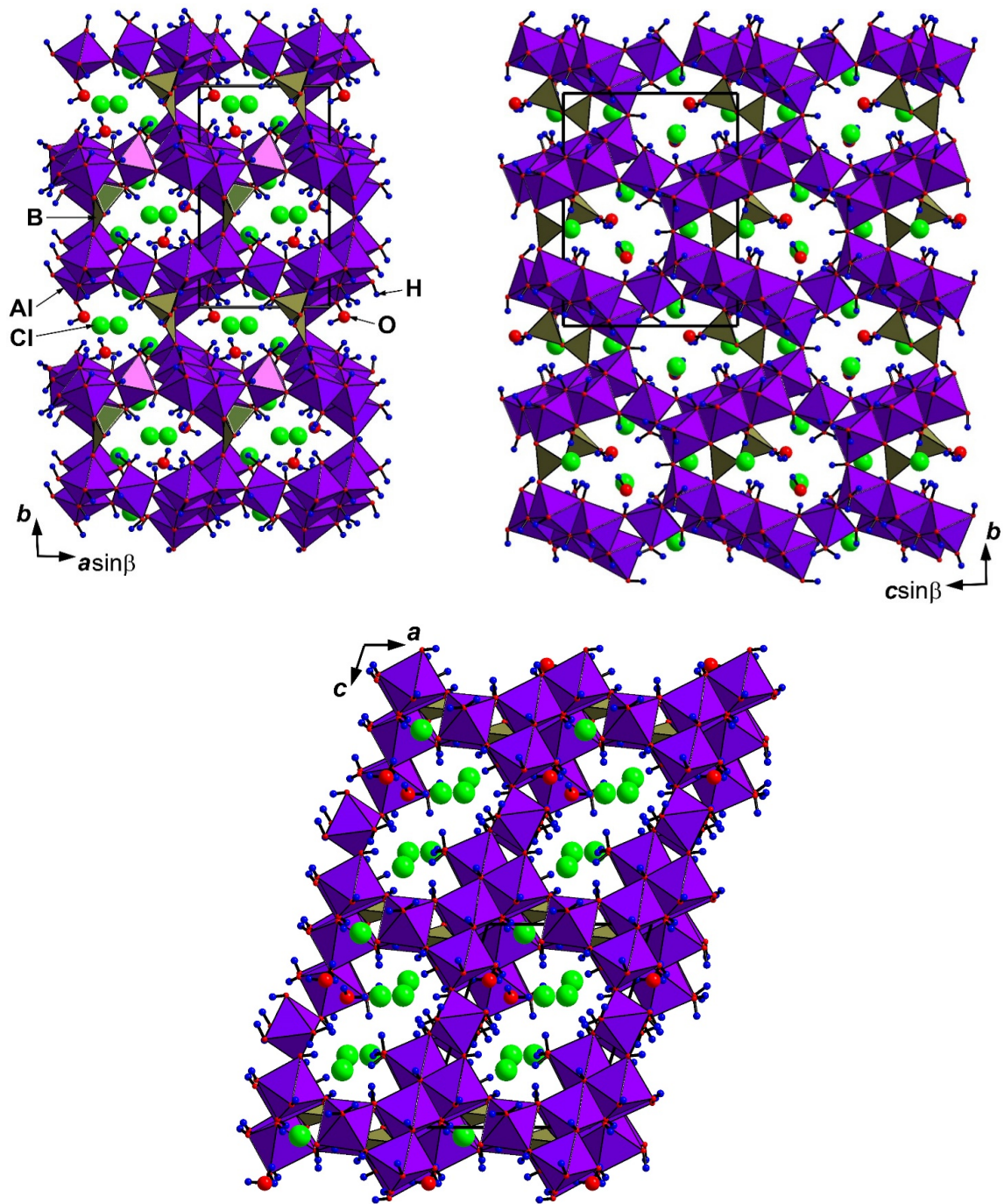


Figure 2. The crystal structure of krasnoshteinite in three projections. The unit cell is outlined.

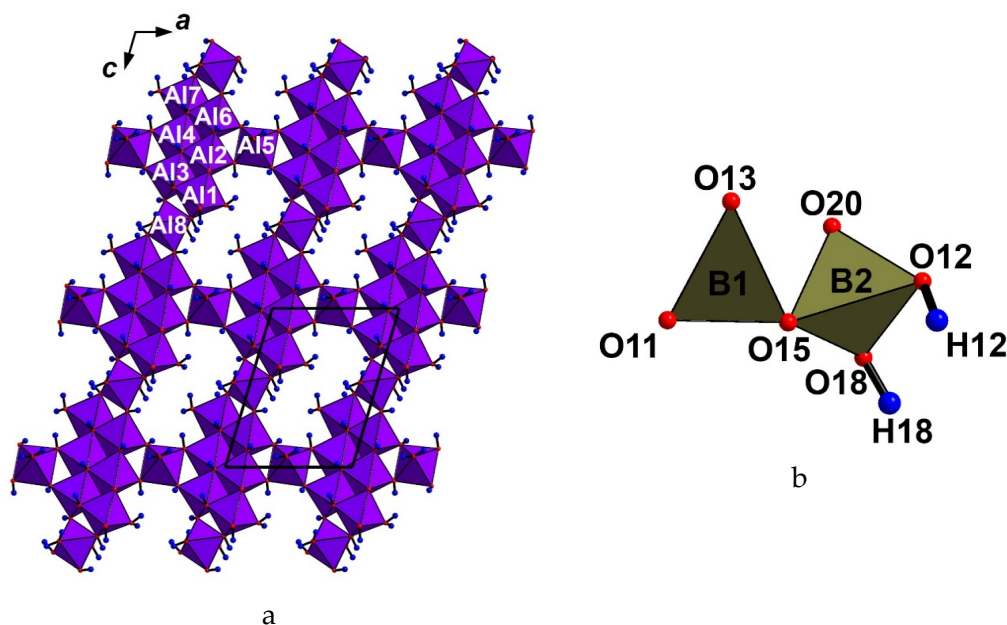


Figure 3. Octahedral layer (a) and insular $[B_2O_4(OH)_2]^{4-}$ group (b) in the structure of krasnoshteinite. For legend, see Table 3.

5. Conclusions

This paper is devoted to the new mineral species, krasnoshteinite. No mineral or synthetic compound related to it, in terms of crystal structure, has been found in literature and databases. Krasnoshteinite contains an earlier unknown borate polyanion, the insular $[B_2O_4(OH)_2]^{4-}$ group consisting of one BO_3 triangle and one $BO_2(OH)_2$ tetrahedron sharing corner. It was a surprise that such a simple anionic complex turned out novel for borates, both natural and synthetic, which is one of the most structurally diverse and best-studied classes of chemical compounds.

Krasnoshteinite ($Al_8[B_2O_4(OH)_2](OH)_{16}Cl_4 \cdot 7H_2O$) is the second, after jeremejevite ($Al_6(BO_3)_5(F,OH)_3$), natural borate with only Al as a metal cation; and the second, after satimolite ($KNa_2(Al_5Mg_2)[B_{12}O_{18}(OH)_{12}](OH)_6Cl_4 \cdot 4H_2O$), mineral with a zeolite-like aluminoborate framework motif in the structure. Due to the presence of a three-dimensional system of wide channels containing Cl^- anions and weakly bonded H_2O molecules, krasnoshteinite is of interest as a potential prototype of a novel family of microporous crystalline materials without large cations.

Borate minerals with species-defining Al formed in high-temperature and low-temperature geological formations are strongly different in crystal chemistry and physical and chemical properties. The high-temperature Al borates and oxoborates do not contain H_2O molecules, have compact crystal structures, and are typically characterized by high hardness and mechanical and chemical stability. Their crystal structures contain only one type of B-centered polyhedral, BO_3 triangles, or BO_4 tetrahedra. Unlike them, the low-temperature Al borates are highly hydrated, have low hardness, and are chemically unstable. They contain complex borate polyanions composed of both triangular and tetrahedral borate polyhedra with OH groups which participate in boron tetrahedra. Their structures are zeolite-like, being based upon open-work aluminoborate motifs.

Supplementary Materials: The following are available online at <http://www.mdpi.com/2073-4352/10/4/301/s1>.

Author Contributions: Conceptualization, I.V.P., N.V.Z., I.I.C., and D.Y.P.; Methodology, I.V.P., N.V.Z., and S.N.B.; Investigation, I.V.P., N.V.Z., I.I.C., E.P.C., D.I.B., V.O.Y., Y.V.B., and I.L.; Writing—Original Draft Preparation, I.V.P., N.V.Z., I.I.C., and D.Y.P.; Writing—Review and Editing, I.V.P. and N.V.Z.; Visualization, N.V.Z. All authors have read and agreed to the published version of the manuscript.

Funding: This work was supported by the Russian Foundation for Basic Research, grants 18-29-12007-mk (I.V.P., N.V.Z., and V.O.Y. for electron microprobe, XRD, and crystal structure studies) and 18-05-00046 (I.I.C. and E.P.C. for fieldwork and SEM studies).

Acknowledgments: The research has been carried out using facilities at the XRD Research Center of St. Petersburg State University in part of powder XRD study.

Conflicts of Interest: The authors declare no conflict of interest.

References

1. Rudnick, R.L.; Gao, S. The Composition of the Continental Crust. In *Treatise on Geochemistry, 3, The Crust*; Holland, H.D., Turekian, K.K., Eds.; Elsevier-Pergamon: Oxford, UK, 2003.
2. The Official IMA-CNMNC List of Mineral Names. Updated List of IMA-Approved Minerals. Available online: <http://cnmnc.main.jp> (accessed on 5 March 2020).
3. Anovitz, L.M.; Grew, E.S. Mineralogy, petrology and geochemistry of boron: An introduction. In *Boron: Mineralogy, Petrology and Geochemistry. Rev. Mineral.* **1996**, *33*, 1–40.
4. Hawthorne, F.C.; Burns, P.C.; Grice, J.D. The crystal chemistry of boron. In: *Boron: Mineralogy, Petrology and Geochemistry. Rev. Mineral.* **1996**, *33*, 41–115.
5. Ivanov, A.A.; Voronova, M.L. *Verkhnekamskoe Potassium Salt Deposit*; Nedra Publishing: Leningrad, Russia, 1975; pp. 1–219. (In Russian)
6. Kudryashov, A.I. *Verkhnekamskoe Salt Deposit*, 2nd ed.; Epsilon Plus: Moscow, Russia, 2013; pp. 1–368. (In Russian)
7. Zhitova, E.S.; Pekov, I.V.; Chaikovskiy, I.I.; Chirkova, E.P.; Yapaskurt, V.O.; Bychkova, Y.V.; Belakovskiy, D.I.; Chukanov, N.V.; Zubkova, N.V.; Krivovichev, S.V.; et al. Dribsite, $\text{Li}_2\text{Al}_4(\text{OH})_{12}\text{C}_{12}\cdot 3\text{H}_2\text{O}$, a new gibbsite-based hydroxalite-supergroup mineral. *Minerals* **2019**, *9*, 492. [CrossRef]
8. Mandarino, J.A. The Gladstone–Dale compatibility of minerals and its use in selecting mineral species for further study. *Can. Miner.* **2007**, *45*, 1307–1324. [CrossRef]
9. Agilent Technologies. *CrysAlisPro Software System*; Version 1.171.37.35; Agilent Technologies UK Ltd.: Oxford, UK, 2014.
10. Sheldrick, G.M. Crystal structure refinement with SHELXL. *Acta Cryst.* **2015**, *A71*, 3–8.
11. Britvin, S.N.; Dolivo-Dobrovolsky, D.V.; Krzhizhanovskaya, M.G. Software for processing of X-ray powder diffraction data obtained from the curved image plate detector of Rigaku RAXIS Rapid II diffractometer. *Zap. Rmo.* **2017**, *146*, 104–107. (In Russian with English Abstract)
12. Bruker-AXS. *Topas V4.2: General Profile and Structure Analysis Software for Powder Diffraction Data*; Bruker: Karlsruhe, Germany, 2009.
13. Nespolo, M.; Ferraris, G. Twinning by syngonic and metric merohedry. Analysis, classification and effects on the diffraction pattern. *Zeit. Krist.* **2000**, *215*, 77–81. [CrossRef]
14. Brese, N.E.; O’Keeffe, M. Bond-valence parameters for solids. *Acta Crystallogr.* **1991**, *B47*, 192–197. [CrossRef]
15. Ferraris, G.; Ivaldi, G. Bond Valence vs. Bond Length in O···O Hydrogen Bonds. *Acta Cryst.* **1988**, *B44*, 341–344. [CrossRef]
16. Malcherek, T.; Schlüter, J. $\text{Cu}_3\text{MgC}_{12}(\text{OH})_6$ and the bond-valence parameters of the OH-Cl bond. *Acta Cryst.* **2007**, *B63*, 157–160. [CrossRef] [PubMed]
17. Burns, P.C.; Grice, J.D.; Hawthorne, F.C. Borate minerals. I. Polyhedral clusters and fundamental building blocks. *Can. Miner.* **1995**, *33*, 1131–1151.
18. Grice, J.D.; Burns, P.C.; Hawthorne, F.C. Borate minerals. II. A hierarchy of structures based upon the borate fundamental building block. *Can. Miner.* **1999**, *37*, 731–762.
19. Gao, W.; Wang, Y.; Li, G.; Liao, F.; You, L.; Lin, J. Synthesis and Structure of an Aluminum Borate Chloride Consisting of 12-Membered Borate Rings and Aluminate Clusters. *Inorg. Chem.* **2008**, *47*, 7080–7082. [CrossRef] [PubMed]
20. Ju, J.; Yang, T.; Li, G.; Liao, F.; Wang, Y.; You, L.; Lin, J. PKU-5: An Aluminoborate with Novel Octahedral Framework Topology. *Chem. Eur. J.* **2004**, *10*, 3901–3906. [CrossRef] [PubMed]
21. Yang, T.; Ju, J.; Li, G.; Liao, F.; Zou, X.; Deng, F.; Chen, L.; Su, J.; Wang, Y.; Lin, J. Square-Pyramidal/Triangular Framework Oxide: Synthesis and Structure of PKU-6. *Inorg. Chem.* **2007**, *46*, 4772–4774. [CrossRef] [PubMed]
22. Pekov, I.V.; Zubkova, N.V.; Ksenofontov, D.A.; Chukanov, N.V.; Yapaskurt, V.O.; Korotchenkova, O.V.; Chaikovskiy, I.I.; Bocharov, V.M.; Britvin, S.N.; Pushcharovsky, D.Y. Redefinition of satimolite. *Miner. Mag.* **2018**, *82*, 1033–1047. [CrossRef]

23. Chen, H.; Ju, J.; Meng, Q.; Su, J.; Lin, C.; Zhou, Z.; Li, G.; Wang, W.; Gao, W.; Zeng, C.; et al. PKU-3: An HCl-Inclusive Aluminoborate for Strecker Reaction Solved by Combining RED and PXRD. *J. Am. Chem. Soc.* **2015**, *137*, 7047–7050. [[CrossRef](#)] [[PubMed](#)]
24. Anthony, J.W.; Bideaux, R.A.; Bladh, K.W.; Nichols, M.C. *Handbook of Mineralogy. Vol. V. Borates, Carbonates, Sulfates*; Mineral Data Publishing: Tucson, AZ, USA, 2003; pp. 1–813.
25. Pekov, I.V.; Zubkova, N.V.; Yapaskurt, V.O.; Ksenofontov, D.A.; Chaikovskiy, I.I.; Korotchenkova, O.V.; Chirkova, E.P.; Pushcharovsky, D.Y. Towards structural mineralogy and genetic crystal chemistry of boron: Novel crystal structures of borate and borosilicate minerals from different geological formations. In Proceedings of the XIX International Meeting on Crystal Chemistry, X-ray Diffraction and Spectroscopy of Minerals, Apatity, Russia, 2–6 July 2019; p. 98.



© 2020 by the authors. Licensee MDPI, Basel, Switzerland. This article is an open access article distributed under the terms and conditions of the Creative Commons Attribution (CC BY) license (<http://creativecommons.org/licenses/by/4.0/>).